

Epileptic seizures in a bistable regime

September 15, 2022

P. R. Protachevicz¹, F. S. Borges², E. L. Lameu³, P. Ji^{4,5}, K. C. Iarosz⁶, A. H. Kihara², I. L. Caldas⁶, J. D. Szezech Jr^{1,7}, M. S. Baptista⁸, A. M. Batista^{1,7,*}

¹Graduate in Science Program - Physics, State University of Ponta Grossa, PR, Brazil.

²Center for Mathematics, Computation, and Cognition, Federal University of ABC, São Bernardo do Campo, SP, Brazil.

³National Institute for Space Research, São José dos Campos, SP, Brazil.

⁴Institute of Science and Technology for Brain-Inspired Intelligence, Fudan University, Shanghai, China.

⁵Key Laboratory of Computational Neuroscience and Brain-Inspired Intelligence, Fudan University, Ministry of Education, China.

⁶Institute of Physics, University of São Paulo, São Paulo, SP, Brazil.

⁷Department of Mathematics and Statistics, State University of Ponta Grossa, Ponta Grossa, PR, Brazil.

⁸Institute for Complex Systems and Mathematical Biology, SUPA, University of Aberdeen, Aberdeen, Scotland, United Kingdom.

*Corresponding author: antoniomarcosbatista@gmail.com

Abstract

Abnormal synchronisation has been associated with epileptic seizures, one of the most common brain disease. Due to this fact, a better understanding of neuronal synchronisation mechanisms can help in the epilepsy treatment. We study neuronal synchronisation by means of a randomly network with excitatory and inhibitory synapses, where the neuron model is given by the adaptive exponential integrate-and-fire. In our network, we verify that the decrease in the influence of inhibition can generate synchronisation from a pattern of desynchronised spikes. The transition from desynchronous spikes to synchronous bursts activities, induced by varying the synaptic coupling, emerges in a hysteretic loop due to a bistable regime where normal (desynchronous) or abnormal (synchronous) regimes exist. We show that, for parameters within the bistable region, a square current pulse can trigger the

abnormal synchronous regime, a process we claim to reproduce features of an epileptic seizure. We can also suppress it, as well. Suppression can be achieved through a current with small amplitude applying on less than 10% of neurons. Therefore, our results demonstrate that electrical stimulation not only can trigger synchronous behaviours, but also can be an effective treatment for epileptic seizures induced in a bistable regime.

Keywords: neuronal network, unbalanced network, epilepsy, bistability

1 Introduction

Epilepsy is a brain disease that causes seizures and sometimes loss of consciousness. Epileptic seizures are associated with synchronous activities [1, 2, 3] of some neocortex regions or other neuronal populations [4, 5, 6, 7, 8]. Electroencephalography has been used to identify and classify seizures [9], as well as to understand epileptic seizures [10]. Abnormal activities have a short period of time, lasting for a few seconds or minutes [11], and they can occur in small or large regions [12, 13]. Two suggested mechanisms to generate partial epilepsy are the decreasing of inhibition and increasing of excitation [12]. In experiments and simulations, the reduction of excitatory and the increase of inhibitory influence have been effective to suppress and prevent synchronised behaviours [14, 15]. Traub and Wong [16] showed which the synchronised bursts that appears in an epileptic seizure is dependent on the neuronal dynamics.

A single seizure could not kill neurons, however recurrent seizures could kill neurons and lead to chronic epilepsy [17]. There are evidences of seizures due to abnormal anatomical alterations, such as mossy fiber sprouting [18], dendritic reconfigurations [19, 20], and neurogenesis [21, 22]. The alterations change the balance between inhibition and excitation [23, 24]. Wang et al. [25] showed that a small alteration in the neuronal network topology can induce a bistable state with abrupt transition to synchronisation. Some *in vitro* seizures generated epileptiform activities when inhibitory synapses were blocked or excitatory synapses were enhanced [26, 27]. Studies have showed that epilepticform activities are related not only with unbalanced neuronal networks, but also with high synchronous regimes [28, 29].

Different routes to epileptic seizures were reported by Silva et al. [24]. They considered the epilepsy as a dynamical disease and presented a theoretical framework where the epileptic seizures occur in neuronal networks that exhibit bistable dynamics. In the bistable state, transitions can happen between desynchronous and synchronous behaviours. Suffczynski et al. [30] modelled the dynamics of epileptic phenomena by means of a bistable

neuronal network.

Many works reported that periodic electrical pulse stimulation facilitates the synchronisation while random stimulation promotes desynchronisation in neuronal network [31]. Electrical stimulation can be applied in different brain areas, for instance hippocampus, thalamus, and cerebellum [12]. The mechanism of the electrical stimulation to cease seizures is not completely known, however, signal parameters such as frequency, duration, and amplitude can be changed to improve the efficiency of treatment for epilepsy [12]. The electrical stimulation has been used as an efficient treatment for hippocampal epileptic [32].

In this work, we build a neuronal network to study epileptic seizures induced in a bistable state. We consider a random network that is composed of adaptive exponential integrate-and-fire (AEIF) neurons coupled by means of inhibitory and excitatory synapses. The AEIF mimics phenomenological behaviours of neurons [33], and it is appropriate to study large networks [34]. Borges et al. [35] verified that depending on the excitatory synaptic strength and the connection probability, a random network of coupled AEIF exhibits transitions between desynchronised spikes and synchronised bursts [36]. In our neuronal network, we observe the existence of bistability when it is unbalanced, namely the decrease of the synaptic inhibition induces a bistable state. We analyse the effects of an external square current pulse (SCP) perturbing the network set with parameters leading to a bistable state. We show that, depending on the duration and amplitude, the SCP can trigger or suppress the synchronisation in the bistability region.

2 Neuronal network model

We build a random network composed of $N = 1000$ adaptive exponential integrate-and-fire neurons with probability of connections $p = 0.1$ [37]. This network has 80% of excitatory and 20% of inhibitory neurons. In the network, the dynamics of each neuron i is given by

$$\begin{aligned}
 C \frac{dV_i}{dt} &= -g_L(V_i - E_L) + g_L \Delta_T \exp\left(\frac{V_i - V_T}{\Delta_T}\right) \\
 &+ I_i - w_i + \sum_{j=1}^{n_i} (V_{\text{REV}}^j - V_i) M_{ij} g_j + \Gamma_i, \\
 \tau_w \frac{dw_i}{dt} &= a_i(V_i - E_L) - w_i, \\
 \tau_s \frac{dg_i}{dt} &= -g_i.
 \end{aligned} \tag{1}$$

The membrane potential V_i and the adaptation current w_i are the two variables that represent the state of each neuron i . These variables depend on the some parameters and also with themselves. The capacitance membrane ($C_m = 200$ pF), leak conductance ($g_L = 12$ nS), resting potential ($E_L = -70$ mV), slope factor ($\Delta_T = 2.0$ mV), and spike threshold ($V_T = -50$ mV) determine the time evolution of the potential membrane. The adaptation current depends on the adaptation time constant ($\tau_w = 300$ ms), and level of subthreshold adaptation (a_i randomly distributed in the interval $[0.19, 0.21]$ nS). We consider the injection of current (I_i) for each neuron in terms of the relative rheobase current $r_i = I_i/I_{\text{rheobase}}$ [34]. The rheobase is a minimum amplitude of applied current to generate a single or successive firings. The application of this constant current allows that the neurons change its potential from resting potential and spike. The value of rheobase depends on the neuron parameters. External current arriving to the neuron i is represented by Γ_i . We consider the external current according to a SCP with amplitude A_I and time duration T_I . The connections are described by the adjacency matrix (M_{ij}) which has element with value 1 (0) when there is a connection (no connection) from neuron j to i . The synaptic conductance (g_i), synaptic reversal potential (V_{REV}) and synaptic time constant ($\tau_s = 2.728$ ms) control the excitatory ($V_{\text{REV}} = 0$ mV) and inhibitory ($V_{\text{REV}} = -80$ mV) synapses. N_i corresponds to the number of connections arriving to the neuron i . The synaptic conductance has an exponential decay with a synaptic time constant (τ_s). When the membrane potential of neuron i is above a threshold $V_i > V_{\text{thres}} = 0$, the state variable is update following the rule

$$\begin{aligned}
 V_i &\rightarrow V_r = -58 \text{ mV}, \\
 w_i &\rightarrow w_i + 70 \text{ pA}, \\
 g_i &\rightarrow g_i + g_s,
 \end{aligned} \tag{2}$$

where g_s assumes the g_{exc} value when i is an excitatory neuron ($i \leq 0.8N$) and g_{inh} for inhibitory neurons ($i > 0.8N$). Aiming to study the parameter space related to g_{exc} and g_{inh} we consider a relative inhibitory synaptic conductance defined as $g = g_{\text{inh}}/g_{\text{exc}}$.

3 Dynamics measurements

3.1 Synchronisation

The synchronous behaviour in the neuronal network can be identified by means of the complex phase order parameter [38]

$$R(t) \exp(i\Phi(t)) \equiv \frac{1}{N} \sum_{j=1}^N \exp(i\psi_j), \quad (3)$$

where $R(t)$ and $\Phi(t)$ are the amplitude and the angle of a centroid phase vector over time, respectively. The phase of the neuron j is obtained by means of

$$\psi_j(t) = 2\pi m + 2\pi \frac{t - t_{j,m}}{t_{j,m+1} - t_{j,m}}, \quad (4)$$

where $t_{j,m}$ corresponds to the time of the m th spike of the neuron j ($t_{j,m} < t < t_{j,m+1}$). We consider that the spike occurs for $V_j > V_{\text{thres}} = 0$ mV. $R(t)$ is equal to 1 for completely synchronised regimes and closely to 0 in the completely desynchronised regimes.

We calculate the time-average order-parameter, that is given by

$$\bar{R} = \frac{t_{\text{step}}}{t_{\text{fin}} - t_{\text{ini}}} \sum_{t_{\text{ini}}}^{t_{\text{fin}}} R(t), \quad (5)$$

where $t_{\text{fin}} - t_{\text{ini}}$ is the time window and $t_{\text{step}} = 1$ ms is the time step interval.

3.2 Synaptic input

We monitor the instantaneous synaptic conductances arriving in each neuron i through

$$I_i^{\text{syn}}(t) = \sum_{j=1}^{N_i} (V_{\text{REV}}^j - V_i) M_{ij} g_j. \quad (6)$$

The instantaneous synaptic input changes over time due to the excitatory and inhibitory inputs.

3.3 Coefficient of variation

The m th inter-spike interval ISI_i^m is defined as the difference between two consecutive spikes of the neuron i , namely

$$\text{ISI}_i^m = t_i^{m+1} - t_i^m > 0, \quad (7)$$

where t_i^m is the time of the m th spike of the neuron i .

Using the mean value of ISI $_i$ ($\overline{\text{ISI}}_i$) and the standard deviation (σ_{ISI_i}), we calculate the coefficient of variation (CV)

$$\text{CV}_i = \frac{\sigma_{\text{ISI}_i}}{\overline{\text{ISI}}_i}. \quad (8)$$

The mean value of CV ($\overline{\text{CV}}$) is obtained through

$$\overline{\text{CV}} = \frac{1}{N} \sum_{i=1}^N \text{CV}_i. \quad (9)$$

The CV measure is utilised to identify spike ($\overline{\text{CV}} < 0.5$) and burst firing patterns ($\overline{\text{CV}} \geq 0.5$) [35, 36].

3.4 Instantaneous and mean firing-rate

The instantaneous firing-rate in intervals of 1 ms is given by

$$F(t) = \frac{1}{N} \sum_{i=1}^N \left(\int_t^{t+1\text{ms}} \delta(t - t_i) dt \right), \quad (10)$$

where t_i is the firing time of the neuron i in the time interval $t \leq t_i \leq t + 1$ ms. This measure allows to obtain the instantaneous population activity of the neuronal network. The mean firing-rate for the neuronal network is calculated by means of

$$\overline{F} = \frac{1}{\overline{\text{ISI}}}, \quad (11)$$

where $\overline{\text{ISI}}$ is obtained by the equation $\overline{\text{ISI}} = \frac{1}{N} \sum_{i=1}^N \overline{\text{ISI}}_i$.

4 Inhibitory effect on synchronous behaviour

The balance of excitation and inhibition generates asynchronous activity in our neuronal network [39, 40]. However, for the unbalanced network we observe synchronised spikes and bursts. Figures 1(a), 1(b), and 1(c) show the mean order parameter (\overline{R}), the mean coefficient of variation ($\overline{\text{CV}}$), and the mean firing rate (\overline{F}), respectively, for the parameter space $g \times r$, where g is the ratio between the inhibitory (g_{inh}) and excitatory (g_{exc}) synaptic conductance, and r is the relative rheobase current. For $g_{\text{exc}} = 0.4$ nS and $g > 6$, we observe $\overline{R} < 0.5$ and $\overline{\text{CV}} < 0.5$, corresponding to desynchronised spikes. In Fig. 1(d), we see the raster plot and the membrane potential for

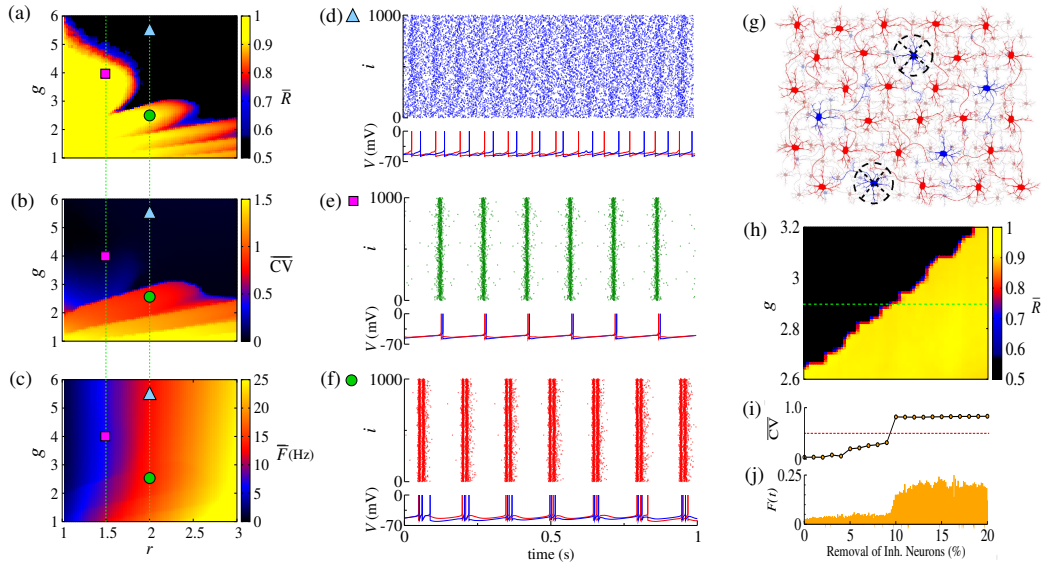


Figure 1: (Colour online) Parameter space $g \times r$ for the mean value of (a) order parameter (\bar{R}), (b) coefficient of variation (\overline{CV}), and (c) firing rate (\bar{F}). Raster plot and membrane potential are shown for (d) desynchronised spikes for $r = 2.0$ and $g = 5.5$ (cyan triangle), (e) synchronised spikes for $r = 1.5$ and $g = 4$ (magenta square), and (f) synchronised bursts for $r = 2.0$ and $g = 2.5$ (green circle). We consider $g_{\text{exc}} = 0.4$ nS. In (g), we illustrate a neuronal network composed of excitatory (red) and inhibitory (blue) neurons, where inhibitory neurons are removed (black dashed circle). Figure (h) shows the time-average order parameter for values of g versus the percentage of inhibitory neurons removed in the network. The green dashed line corresponds to $g = 2.9$. The values of \overline{CV} and instantaneous firing rate are shown in (i) and (j), respectively.

2 neurons in the neuronal network with desynchronised spikes pattern for $g = 5.5$ and $r = 2$ (blue triangle). For $g = 4$ and $r = 1.5$ (magenta square), the network exhibits synchronised spikes (Fig. 1(e)), as a result $\bar{R} > 0.9$ and $\overline{CV} < 0.5$. Figure 1(f) shows synchronised bursts for $g = 2.5$ and $r = 2$ (green circle), where $\bar{R} > 0.9$ and $\overline{CV} > 0.5$. We verify transitions from desynchronised spikes to synchronised bursts without significant change of the mean firing rate value.

The appearance of synchronous behaviour can be not only related to a decreasing of inhibitory synaptic strength, but also to lost of inhibitory neurons. Figure 1(g) illustrates a neuronal network composed of excitatory (red) and inhibitory (blue) neurons, where some inhibitory neurons are removed (dashed circles). In Fig. 1(h), we see that the synchronous behaviour de-

depends on the value of g and the percentage of removed inhibitory neurons. Figures 1 (i) and 1(j) display the transition of spikes ($\overline{CV} < 0.5$) to bursts ($\overline{CV} \geq 0.5$) and the instantaneous firing rate $F(t)$, respectively. For $g = 2.9$ and $g_{\text{exc}} = 0.4$ nS (green dashed line), the transition to synchronised bursts occurs when $\approx 10\%$ of inhibitory neurons are removed out of the neuronal network, and as a consequence $F(t)$ can reach 0.2.

Therefore, alterations in the inhibitory synaptic strength or in the number of inhibitory neurons can induce transitions to synchronous patterns. Wang et al. [25] presented synchronisation transition as a result of small change in neuronal network topology. In this work, we study the transition caused due to changes in the inhibitory synaptic strength and bistable regime emergence.

5 Bistable regime

We analyse the synchronisation using the parameter space $g \times g_{\text{exc}}$. Figure 2(a) exhibits \overline{R} in colour scale. The black region corresponds to desynchronised spike activity, while the other coloured regions are associated with bursts activities. The white region represents the bistable state, where both desynchronised spikes and synchronised bursts are possible depending on the initial conditions. In the bistable regime, when g_{exc} is decreased in the backward direction, \overline{R} is higher than in the forward direction, as shown in Fig. 2(b) for $g = 3$ and $g_{\text{exc}} = [0.35, 0.45]$ nS (green dashed line in Fig. 2(a)). We identify the bistability (white region) in the parameter space parameter when $\overline{R}_{\text{backward}} - \overline{R}_{\text{forward}} > 0.4$. Raster plot and instantaneous synaptic input for desynchronised spikes (blue circle) and synchronised bursts (red square) are shown in Figs. 2(c) and 2(d), respectively. When the neuronal network has desynchronised spikes, the instantaneous synaptic inputs are approximately $I_{\text{syn}}(t) = 100$ pA and are distributed over time. For synchronised bursts, $I_{\text{syn}}(t) \approx 0$ when a large part of the network is not firing, and $I_{\text{syn}}(t) > 200$ pA during synchronous firing activities.

In the bistable regime, we investigate the evolution of the trajectory for a finite time interval in the phase space $w_i \times V_i$ and the time evolution of w_i , as shown in Fig. 3 for $i = 1$, where the gray regions correspond to $dV_i/dt \leq 0$. The gray region frontier is given by $dV_i/dt = 0$, that is the V_i -nullcline [34]. During spikes activities, the trajectory (Fig. 3(a)) and the time evolution of w_i (Fig. 3(b)) do not cross the V_i -nullcline. For bursts activities (Figs. 3(c) and 3(d)), it is observed w_i values in the region $dV_i/dt \leq 0$. The emergence of the bistable behaviour is related to change in the V_i -nullcline caused by the variation of I_{syn} during the spike. For bursts activities the trajectory in the region $dV_i/dt \leq 0$ allows w_1 to be smaller in the first spike and larger in

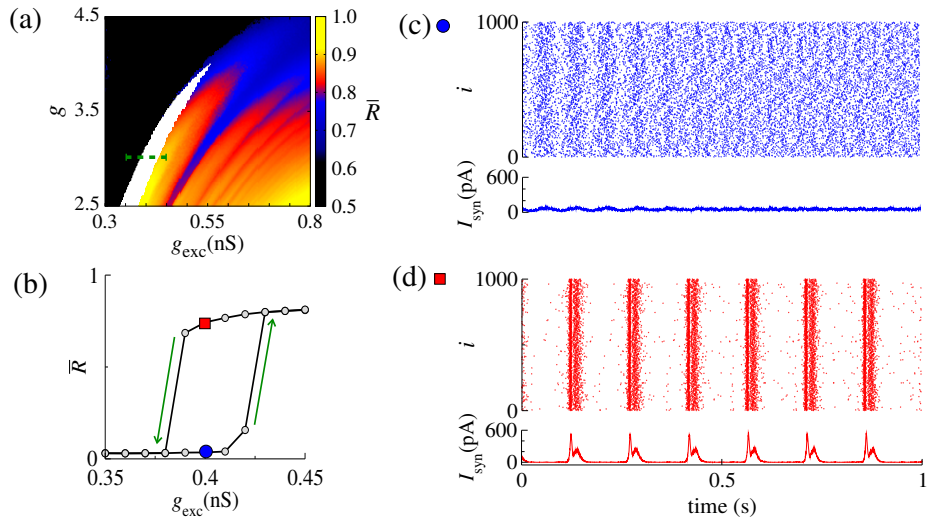


Figure 2: (Colour online) (a) $g \times g_{exc}$, where \bar{R} is encoded in colour. The black region corresponds to the desynchronised activity, coloured regions indicate $\bar{R} > 0.6$, and white region represents the bistable regime. (b) Bistable region indicated in the parameter space of (a) by means of a green dashed line. (c) and (d) show the raster plots and the I_{syn} values for desynchronised spikes (blue circle) and synchronised bursts (red square), respectively.

the second spike. For spikes activities the values of w_1 are equal in all spikes.

6 External square current pulse

We investigate the effect of the SCP on the bistable region. We apply the SCP in the neurons with a time interval T_I and amplitude A_I . After T_I , the SCP is switched off and we analyse the effect on the dynamical behaviour during and after 10 s.

Firstly, we apply the current pulse in all neurons when the network has parameters leading to the bistable regime, and has a desynchronous regime. Figure 4(a) shows the time (colour scale) that the neurons remain in the synchronised pattern after the SCP. In the black region, we see that the external perturbation does not change the dynamical behaviour, namely the neurons remain in a desynchronised spikes. The yellow region displays the values of T_I and A_I of the SCP that change the behaviour of the neurons from desynchronised spikes to synchronised bursts. For one point inside the black region (white circle), we see that the instantaneous firing rate ($F(t)$) defined in Eq 10 (Fig. 4(b), blue line) has irregular oscillations with small

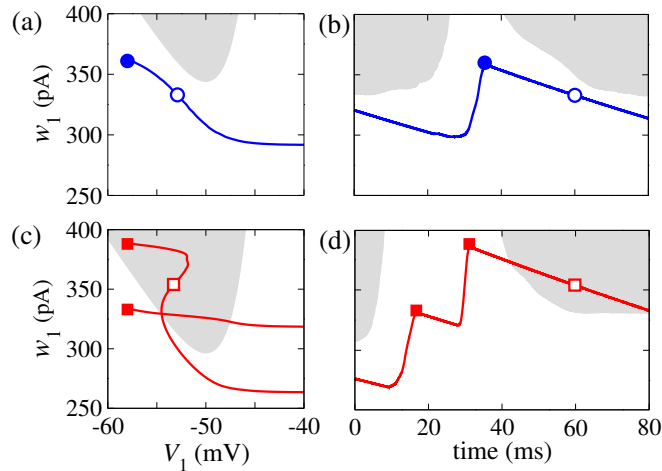


Figure 3: (Colour online) Phase space $w_1 \times V_1$ ((a) and (c)) and time evolution of w_1 ((b) and (d)) for spikes (blue) and bursts activities (red). The gray regions correspond to $dV_1/dt \leq 0$.

amplitude, as a result of desynchronised spikes. For T_I and A_I values inside the yellow region (green square), $F(t)$ exhibits regular oscillation after the application of the SCP, as a consequence of the synchronised bursts. For the parameters in the yellow region, we see that for sufficiently large amplitudes, the change in behaviour induced by the perturbation does not depend on the time. Another relevant observation is that for perturbations with small amplitudes applied for a short time is sufficient to induce synchronous burst activity in the bistable regime. This suggests that even small excitatory stimuli arriving from other brain regions can be sufficient to initiate epileptic seizures.

Secondly, we apply the stimulus when the network has neurons with the synchronised burst in the bistable firing pattern regime. We aim to suppress synchronous behaviour by means of the SCP. We consider a SCP with positive and negative amplitudes being applied on 10% of the neurons in the network. Figure 5(a) shows how long the bursts remain synchronised after the SCP to be switched off (colour bar). We verify that both negative and positive amplitudes exhibit regions where the synchronous behaviours are suppressed, namely there is a transition from synchronised bursts to desynchronised spikes. In addition, for $T_I > 0.4$ s and considering the absolute value of the amplitudes, the transition occurs for positive values with smaller amplitudes than the negative values. In Fig. 5(b), we see the dependence of the percentage of perturbed neurons by the stimulus on the time that the neurons remain in the bursting synchronous regime. So, the black region

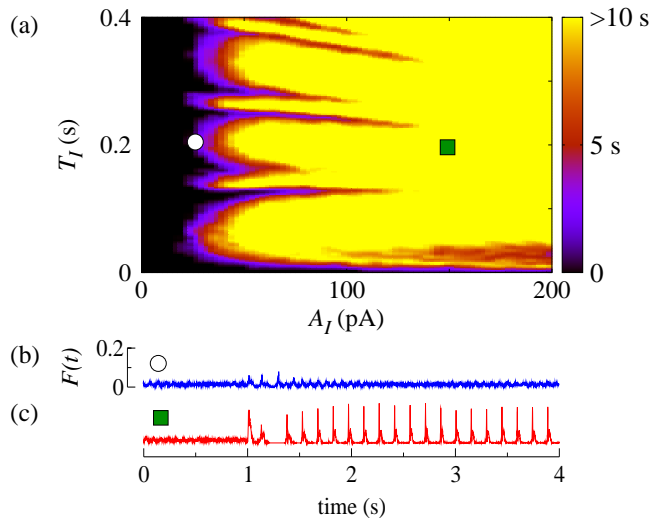


Figure 4: (Colour online) (a) $T_I \times A_I$ in the bistable region. Firing rate for values according to (a) white circle and (c) green square. We consider $g_{\text{exc}} = 0.4$ nS, $g = 3$, and $r = 2$.

represent parameters for which the network does not remain synchronous, and therefore, synchronisation is suppressed. In this figure $T_I = 1$ s. From the location of the black region, we conclude that desynchronous behaviour is achieved for $A_I > 15$ pA and at least 9% of perturbed neurons.

7 Conclusion

We studied the influence of inhibitory synapses on the appearance of synchronised and desynchronised firing patterns in a random network composed of adaptive exponential integrate-and-fire neurons. When the inhibitory influence is reduced by either decreasing the inhibitory synaptic strength or the number of inhibitory neurons, the neuronal network is more likely to exhibit synchronous behaviours. The synchronisation is a consequence of the unbalance between excitatory and inhibitory synaptic influences.

We found parameter sets that lead the network to a bistable regime the neuronal population can either behave in a desynchronous spiking regime or a synchronised bursting regime. Inside the region of parameters leading to this bistable regime, a desynchronous (synchronous) network can be turned into synchronous (desynchronous) one by changing forward (backward) the parameter g_{exc} . The onset of synchronisation is thus hysteretic.

We showed that synchronised bursts, in the bistable regime, can be in-

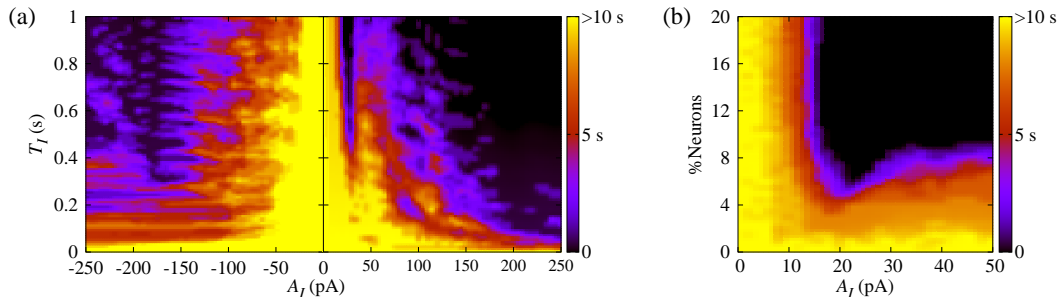


Figure 5: (Colour online) (a) $T_I \times A_I$, where the colour bar indicates the time that the system remains in the synchronized burst behaviour after the SCP. (b) Number of perturbed neurons as a function of A_I . We consider $g_{\text{exc}} = 0.4$ nS, $g = 3$, and $r = 2$.

duced by means of a SCP. However, in our simulations, out of the bistable region, the SCP does not induce a permanent synchronisation. When the neurons are synchronised, in the bistable regime, the SCP can be used to suppress it in the bistability. Positive amplitudes of SCP are more effective to cease the synchronised bursts than negative ones. In addition, our results show that a SCP applied to no more than 10% of neurons is enough to desynchronise the neuronal network.

Our simulations suggest that a decrease of the inhibition contributes to the appearance of epileptic seizure, thus confirming previous experimental results and theoretical models. Both the lost of inhibitory neurons and a decrease in the inhibitory strength induce epilepsy.

From our numerical simulations it is possible to hypothesise that low amplitude stimuli from other parts of the brain would be capable of inducing a seizure in another part of the brain. We can also claim that our results support therapies based on SCP, since we have shown that these perturbations can not only induce but also suppress synchronous behaviour in neuronal networks.

Acknowledgements

This study was possible by partial financial support from the following Brazilian government agencies: CNPq (433782/2016-1), CAPES, and FAPESP (2015/50122-0, 2015/07311-7, 2016/16148-5, 2016/23398-8, 2017/13502-5, and 2017/18977-1). We also wish to thank the Newton Fund and COFAP.

References

- [1] Li, X., Cui, D., Jiruska, P., Fox, J. E., Yao, X., & Jefferys, J. G. (2007). Synchronization measurement of multiple neuronal populations. *J. Neurophysiol.*, 98, 3341-3348.
- [2] Jiruska, P., de Curtis, M., Jefferys, J. G. R., Schevon, C. A., Schiff, S. J., & Schindler, K. (2013). Synchronization and desynchronization in epilepsy: controversies and hypotheses. *Journal Physiological*, 591.4, 787-797.
- [3] Wu, Y., Liu, D., & Song, Z. (2015). Neuronal networks and energy bursts in epilepsy. *Neuroscience*, 287, 175-186.
- [4] Fisher, R. S., van Emde Boas, W., Blume, W., Elger, C., Genton, P., Lee, P., & Engel, J. Jr. (2005). Epileptic seizures and epilepsy: definitions proposed by the International League Against Epilepsy (ILAE) and the International Bureau for Epilepsy (IBE). *Epilepsia*, 46(4), 470-472.
- [5] Sierra-Paredes, G. & Sierra-Marcuño, G. (2007). Extrasynaptic GABA and glutamate receptors in epilepsy. *CNS Neurological Disorders Drug Targets*, 6, 288-300.
- [6] Engel, J. Jr., Thompson, P. M., Stern, J. M., Staba, R. J., Bragin, A., & Mody, I. (2013). Connectomics and epilepsy. *Current Opinion in Neurology*, 26, 186-194.
- [7] Geier, C., & Lehnertz, K. (2017). Which Brain Regions are Important for Seizure Dynamics in Epileptic Networks? Influence of Link Identification and EEG Recording Montage on Node Centralities. *International Journal of Neural Systems*, 27, 1650033.
- [8] Falco-Walter, J. J., Scheffer, I. E., & Fisher, R. S. (2018). The new definition and classification of seizures and epilepsy. *Epilepsy Research*, 139, 73-79.
- [9] Noachtar, S., & Rémi, J. (2009). The role of EEG in epilepsy: a critical review. *Epilepsy & Behavior*, 15, 22-33.
- [10] Scharfman, H. E. & Buckmaster, P. S. (2014). Issues in clinical epileptology: A view from the bench. New York: Springer.

- [11] Trinka, E., Cock, H., Hesdorffer, D., Rossetti, A., Scheffer, I. E., Shinnar, S., Shorvon, S., & Lowenstein, D. H. (2015). A definition and classification of status epilepticus-report of the ILAE task force on classification of status epilepticus. *Epilepsia*, 56, 1515-1523.
- [12] McCandless, D. W. (2012). *Epilepsy: animal and human correlations*. New York: Springer-Verlag.
- [13] Kramer, M. A. & Cash, S. S. (2012). Epilepsy as a disorder of cortical network organization. *Neuroscientist*, 18(4), 360-372.
- [14] Traub, R. D., Miles, R., & Jefferys, J. G. R. (1993). Synaptic and intrinsic conductances shape picrotoxin-induced synchronized after-discharges in the guinea-pig hippocampal slice. *The Journal of Physiology*, 461, 525-547.
- [15] Schindler, K. A., Bialonski, S., Horstmann, M. T., Elger, C. E., & Lehnertz, K. (2008). Evolving functional network properties and synchronizability during human epileptic seizures. *Chaos*, 18, 033119.
- [16] Traub, R. D. & Wong, R. K. S. (1982). Cellular mechanism of neuronal synchronization in epilepsy. *Science*, 216, 745-747.
- [17] Dingledine, R., Varvel, N. H., & Dudek, F. E. (2014). When and how do seizures kill neurons, and is cell death relevant to epileptogenesis? *Advances in Experimental Medicine and Biology*, 813, 109-122.
- [18] Danzer, S. (2017). Mossy fiber sprouting in the epileptic brain: Taking on the Lernaean Hydra. *Epilepsy Currents*, 17(1), 50-51.
- [19] Wong, M. (2005). Modulation of dendritic spines in epilepsy: Cellular mechanisms and functional implications. *Epilepsy & Behavior*, 7, 569-577.
- [20] Wong, M. (2008). Stabilizing dendritic structure as a novel therapeutic approach for epilepsy. *Expert Review of Neurotherapeutics*, 8(6), 907-915.
- [21] Jessberger, S. & Parent, J. M. (2015). Epilepsy and adult neurogenesis. *Cold Spring Harbor Perspectives in Biology*, 7, 1-10.
- [22] Cho, K.-O., Lybrand, Z. R., Ito, N., Brulet, R., Tafacory, F., Zhang, L., Good, L., Ure, K., Kernie, S. G., Birnbaum, S. G., Scharfman, H.

- E., Eisch, A. J., & Hsieh, J. (2015). Aberrant hippocampal neurogenesis contributes to epilepsy and associated cognitive decline. *Nature Communications*, 6, 6606.
- [23] Holt, A. B. & Netoff, T. I. (2013). Computational modeling of epilepsy for an experimental neurologist. *Experimental Neurology*, 244, 75-86.
- [24] Silva, F. H. L., Blanes, W., Kalitzin, S. N., Parra, J., Suffczynski, P., & Velis, D. N. (2003). Dynamical diseases of brain systems: different routes to epileptic seizures. *IEEE Transactions on Biomedical Engineering*, 50, 540-548.
- [25] Wang, Z., Tian, C., Dhamala, M., & Liu., Z. (2017). A small change in neuronal network topology can induce explosive synchronization and activity propagation in the entire network. *Scientific Reports*, 7, 561.
- [26] Traub, R. D., Jefferys, J. G. R., & Whittington, M. A. (1994). Enhanced NMDA conductance can account for epileptiform activity induced by low Mg²⁺ in the rat hippocampal slice. *Journal of Physiology*, 478, 379-393.
- [27] White, H. S. (2002). Animal models of epileptogenesis, *Neurology*, 59, 7-14.
- [28] Uhlhaas, P. J. & Singer, W. (2006). Neural synchrony in brain disorders: relevance for cognitive dysfunctions and pathophysiology. *Neuron*, 52, 155-168.
- [29] Abdullahi, A. T. & Adamu, L. H. (2017). Neuronal network models of epileptogenesis, *Neurosciences*, 22(2), 85-93.
- [30] Suffczynski, P., Kalitzin, S., & Da Silva, F. H. L. (2004). Dynamic of non-convulsive epileptic phenomena modeled by a bistable neuronal network. *Neuroscience*, 126, 467-484.
- [31] Cota, V. R., Medeiros, D. C., Vilela, M. R. S. P., Doretto, M. C., & Moraes, M. F. D. (2009). Distinct patterns of electrical stimulation of the basolateral amygdala influence pentylentetrazole seizure outcome. *Epilepsy & Behavior*, 14, 26-31.
- [32] Velasco, A. L., Velasco, F., Velasco, M., Trejo, D., Casto, G., & Carrillo-Ruiz, J. D. (2007). Electrical stimulation of the hippocampal epileptic foci for seizure control: a double-blind, long-term follow-up study. *Epilepsia*, 48(10), 1895-1903.

- [33] Clopath, C., Jolivet, R., Rauch, A., Lüscher, H.-R., & Gerstner, W. (2007). Predicting neuronal activity with simple models of the threshold type: adaptive exponential integrate-and-fire model with two compartments. *Neurocomputing*, 70(10-12), 1668-1673.
- [34] Naud, R., Marcille, N., Clopath, C., & Gerstner, W. (2008). Firing patterns in the adaptive exponential integrate-and-fire model. *Biological Cybernetics*, 99, 335-347.
- [35] Borges, F. S., Protachevicz, P. R., Lameu, E. L., Bonetti, R. C., Iarosz, K. C., Caldas, I. L., Baptista, M. S., & Batista, A. M. (2017). Synchronised firing patterns in a random network of adaptive exponential integrate-and-fire neuron model. *Neural Networks*, 90, 1-7.
- [36] Protachevicz, P. R., Borges, R. R., Reis, A. S., Borges, F. S., Iarosz, K. C., Caldas, I. L., Lameu, E. L., Macau, E. E. N., Viana, R. L., Sokolov, I. M., Ferrari, F. A. S., Kurths, J., & Batista, A. M. (2018). Synchronous behaviour in network model based on human cortico-cortical connections. *Physiological Measurement*, 39(7), 074006.
- [37] Brette, R. & Gerstner, W. (2005). Adaptive exponential integrate-and-fire model as an effective description of neuronal activity. *Journal of Neurophysiology*, 94, 3637-3642.
- [38] Kuramoto, Y (1984). Chemical oscillations, waves, and turbulence. Berlin: Springer-Verlag.
- [39] Lundqvist, M., Compte, A., & Lansner, A. (2010). Bistable, irregular firing and population oscillations in a modular attractor memory network. *Plos Computational Biology*, 6(6), e1000803.
- [40] Ostojic, S. (2014). Two types of asynchronous activity in networks of excitatory and inhibitory spiking neurons. *Nature Neuroscience*, 17, 594-600.